Research Square

Preprints are preliminary reports that have not undergone peer review.
They should not be considered conclusive, used to inform clinical practice,
or referenced by the media as validated information.

Rfd1, A Restorer to the Aegilops Juvenalis Cytoplasm, Functions in Fertility Restoration of Wheat Cytoplasmic Male Sterility

Fuqiang Niu
Northwest A&F University: Northwest Agriculture and Forestry University
Yaning Bu
Northwest A&F University: Northwest Agriculture and Forestry University
Xuetong Yang
Northwest A&F University: Northwest Agriculture and Forestry University
Yongfeng Wu
Northwest A&F University: Northwest Agriculture and Forestry University
Mengting He
Northwest A&F University: Northwest Agriculture and Forestry University
Lingli Zhang
Northwest A&F University: Northwest Agriculture and Forestry University
xiyue song (songxiyue@nwafu.edu.cn)
Northwest Agriculture and Forestry University https://orcid.org/0000-0001-8158-3380

Research Article

Keywords: Aegilops Juvenalis, cytoplasmic male sterility,restoration of fertility, hybrid wheat, pectinesterase

Posted Date: March 3rd, 2022

DOI: https://doi.org/10.21203/rs.3.rs-1385182/v1

License: This work is licensed under a Creative Commons Attribution 4.0 International License.
Read Full License

Abstract

Cytoplasmic male sterility (CMS) is a crucial means for the utilization of heterosis, which is of great significance for improving the yield and quality of hybrids. Currently, fertility restorationhas been extensively investigated in crops, but fertility restoration of CMS wheat with *Aegilops Juvenalis* cytoplasm are poorly understood.Here, a backcross population BC_1F_1derived from a cross between male sterile line Ju706A, its maintainer line 706B, and restorer line LK783, was used to map *Rfd1*locus by bulked segregant analysis and wheat 660K SNP genotyping.In which Ju706A displayedcomplete male sterility,and its fertility can be restored by LK783 with a pair of dominant genes *Rfd1Rfd1*. The locus was located to 2.4-Mb region on chromosome 1BS by markers*AX-174254104* and *AX-111201011*.Combined with transcriptomic analysis and quantitative real-time PCR assay,*TraesCS1B02G197400LC*, the most likely candidate gene for *Rfd1*, encoded a pectinesterase which was localized in the cell wall, and was highly expressed in fertile anthers.The silencing of *Rfd1* resulted in decreased fertility and heterogeneous expression of *Rfd1* promoted pollen germination and affected the vegetative growth.It implies that *Rfd1* is required for anther or pollen development and male fertility in CMS wheat with *Aegilops Juvenalis* cytoplasm. Further, a 7 bp deletion in Ju706A was employed to develop specific marker *Xnwafu1* for molecular marker-assisted selection of restorers. Thestudy providesa new understanding for exploring the fertility restoration mechanism of CMS.

Key Message

Rfd1, a restorer locus for *Aegilops Juvenalis* cytoplasm in wheat,was fine mapped in a 2.4-Mb region harboring a pectinesterase gene *TraesCS1B02G197400LC* that may be responsible for fertility restoration.

Introduction

Heterosis, or hybrid vigor is widespread in the biological world and plays an important role in improving wheat yield. Male sterility, as an effective and economical approach, is of significance in the utilization of heterosis (Huang et al. 1990). According to the pattern of inheritance, male sterility can be divided into cytoplasmic male sterility (CMS) and genic male sterility (GMS) (Han et al. 2018). CMS manifested as maternal inheritance, relating to the function of mitochondrial genes, and its fertility can be restored by restorer genes (Hanson and Bentolila 2004; Horn 2006; Tan et al. 2011; Feng et al. 2015). In contrast, GMS is controlled by dominant or recessive nuclear genes, which is involved in development of male gametes, affecting male fertility (Tang et al. 2006; Ke et al. 2010; Fox et al. 2017). CMS is easier to identify maintainer lines compared with GMS, and widely used in many crops, including wheat.

CMS with different types containing T -type, P- type, K -type, V -type, Q -type, S- type, and D^2- type has been extensively researched in wheat (Tsunewaki et al. 1976; Panayotov 1980; Zhang et al. 1987, 1989; Mohr 1993; Murai and Tsunewaki 1993; Sun 2001). Among them, D^2-CMS with *Ae. juvenalis* cytoplasm (designed as Ju-CMS) possessing the characteristics of strong recovery and strong resistance to wheat

powdery mildew has great potential value in improving the production of hybrid wheat (Zhang et al. 2002). However, the systematic research of CMS line with *Ae. Juvenalis* cytoplasm remains unclear.

Parallel with the discovery of CMS line in wheat, fertility restorer genes have also been studied. In T-CMS, eleven major fertility restorer (*Rf*) genes, named *Rf1-Rf11* in turn, have been successfully identified on chromosomes 1A, 7D, 1B, 6B, 6D, 5D, 7B, 5A, 4D, 4A, and 5B (Liu et al. 1999). In particular, *Rf1* and *Rf3* as fertility-restorer genes bind to the mitochondrial *orf279* transcript and induce cleavage, preventing expression of the CMS trait (Melonek et al. 2021). In K-CMS, the fertility gene *Rfk1* is located on chromosomes 1BS and the distance is 34.4 ± 3.8cM between the *Rfk1* and the centromere through the analysis of the telomeres in Chinese Spring wheat (Tsunewaki 1978; Hamawaki et al. 1980). Furthermore, fertility restorer genes, *Rfv1*, *Rfm1* and *Rfn1* in *Aegilops kotschyi*, *Ae. mutica* and *Ae. uniaristata* cytoplasm, respectively, may share the same locus on chromosomes 1BS, the locus is designated Rf^{multi} (Tsunewaki 2015). Recently, the *Rfk1* is delimited within physical intervals of 26.0 Mb by BSR-Seq (chen et al. 2021). Although the phenomenon of D^2-CMS was studied (Murai and Tsunewaki 1995; Zhang and Huang 1997), there are few studies on mapping and cloning of restoring genes for D^2-CMS, especially for the cytoplasmic male sterility of *Ae. juvenalis*.

Pectin is one of the components of plant cell wall and plays an indispensable role in plant growth and development. Pectinesterase (PME) affects the balance of plasticity and mechanical strength that is essential for cell wall and pollen tube growth by modulating the pectin esterification-deesterification degree (Jiang et al. 2005; Tian et al. 2006). Studies have found that plant cell swelling is caused by the partial autolysis of the cell wall promoted by PME (Richard and Noat 1986). In tomato, *Pmeu1*, which encodes a salt-dependent PME, plays a crucial role in cell wall strength (Gaffe et al. 1997). In Chinese cabbage, *BcPME37c*, which is highly expressed in the stamens and its protein is localized in the cell wall, is remarkably important in the formation of the pollen wall (Xiong et al. 2019). In tobacco, exogenous PME can thicken the apical cell wall to inhibit pollen tube growth (Bosch et al., 2005a). PME by interacting with pectin methylesterase inhibitors (PMEI) to maintain cell wall plasticity and regulation pollen development. (Shi and Yang 2010). PME genes have been studied in rice (Yang et al. 2013), tomato (Nogueirol et al. 2015), citrus (Guo et al. 2018), maize (Zhang et al. 2018), banana (Muhammad et al. 2019), whereas their detailed functions in wheat remains unclear.

In this study, Ju-CMS line Ju706A and restoring line LK783 were used to construct backcrossing population Ju706A//LK783/706B and the restorer *Rfd1* was mapped by combining BSA with wheat 660K SNP array genotyping. *TraesCS1B02G197400LC* was identified as a strong candidate gene for *Rfd1* by RNA-Seq and qRT-PCR analysis. Furthermore, barley stripe mosaic virus-induced gene silencing (BSMV-VIGS) and gene overexpression experiments were performed to verify the function of *Rfd1*. Finally, *Xnwafu1* molecular marker was developed for marker-assisted selection. Our work lays a certain theoretical foundation for understanding the fertility restoration mechanism of cytoplasmic male sterility in wheat. Moreover, it also provides solid theoretical and technical support for the production practice of hybrid wheat.

Materials And Methods

Plant materials

Male sterile line Ju706A, maintainer line 706B and the restorer line LK783 and Ju783R were used as research materials. Ju706A is a Ju-CMS line with *Aegilops Juvenalis* cytoplasm. 706B has the cytoplasm of common wheat and the same nuclear background as Ju706A. LK783 is a wheat line with strong fertility recovery ability against *Ae. Juvenalis* cytoplasm (Liu et al. 2002). These materials were used to construct genetic mapping populations. In May 2017, the hybrid combination LK783/706B was formulated and the progeny BC_1F_1 (Ju706A //LK783/706B) population was obtained in May 2019. Finally, a total of 506 plants were obtained and were used to fine map of restorer gene. Ju783R, a restorer line with *Aegilops Juvenalis* cytoplasm and the same nuclear background as LK783, carries the restorer *Rfd1Rfd1*. Ju783R was used for BSMV-VIGS, grown in an artificial climate box under long-day conditions (14 h: 10 h day: night at 25°C). Moreover, 203 restorer lines, 41 maintainer lines and 293 materials from different regions of China were used for molecular marker-assisted selection. All the above materials were grown in Yangling (108° E, 34°15' N), China.

Colombian ecotype (Col-0) *Arabidopsis thaliana* and transgenic plants were used for gene overexpression analysis, grown in an artificial climate box under long-day conditions (16 h: 8 h day: night at 22°C). *Nicotiana benthamiana* was used for subcellular localization, planted in an artificial climate box under long-day conditions (16 h: 8 h day: night at 26°C).

Phenotype identification

During the Tns, the florets and anthers were collected to observe morphological characteristics in stereomicroscope (Motic, K4000). Pollen grains were stained with 1% I_2-KI solution, DAPI solution, aniline blue solution and photographed by stereomicroscope (Motic, K4000). In addition, anthers from male sterile and fertile plants were collected and immersed into glutaraldehyde solution, SEM and TEM were performed as described by (Liu et al. 2018). SEM and TEM images were collected using the scanning electron microscopy (JSM-6360LV, JEOL) and transmission electron microscope (JEM-1230, JEOL), respectively.

DNA extraction and Bulked segregant analysis

Total genomic DNA of Ju706A, LK783 and BC_1F_1 individuals was extracted from fresh leaves using cetyltrimethyl ammonium bromide (CTAB) protocol with some modifications (Han et al. 2015). According to the result of the fertility survey in the BC_1F_1 segregation population, sterile gene pool (SP) and fertile gene pool (FP) were constructed using the bulked segregant analysis (BSA) method. 20 extremely sterile plants with 0% seed setting rate were selected to form SP and 20 extremely fertile plants with seed setting rate more than 85% were selected to form FP. The SP, FP and two parents were used to screen polymorphic molecular markers and acquire sequencing data via 660K SNP arrays.

660K SNP array genotyping and identification of candidate SNPs

The two bulked DNA pools and the two parents were genotyped by 660K SNP arrays at Capitalbio Technology Co. (Beijing; http://www.capitalbiotech.com). The original scan results of the SNP array were genotyped using AAS from Affymetrix or GenomeStudio from Illumina. Based on the genome-wide SNP genotyping results, quality control of SNPs was performed to obtain high-quality SNPs. Dish QC was used for quality control and samples with dish QC higher than 0.82 were used for subsequent analysis. The fertility restorer gene was mapped based on high-quality SNPs and BSA methods. Moreover, the proportion of differential SNPs in each chromosome was calculated after quality control. The experiment was performed in two biological replicates.

SSR and SNP primers design

Primers for SSR markers were designed using the Primer Server tool available through the Triticeae Multi-omics Center (http://202.194.139.32/PrimerServer/) and SNP markers were designed with BatchPrimer3 v1.0 (https://probes.pw.usda.gov/batchprimer3/) (Table S3). Before screening the markers in BC_1F_1 populations, the SSR markers and SNP markers were used to identify polymorphisms between two parents and two pools. The PCR amplification conditions were as follows: 94°C for 5 min; followed by 35 cycles of 94°C for 50 s, 60°C for 50 s, 72°C for 1min; and 72°C for 10 min. The PCR products were tested on polyacrylamide gel electrophoresis (PAGE) (Han et al. 2015) and silver stained (Liang et al. 2014). According to the obtained polymorphic markers and the recombinant plants, the genetic linkage map was drawn using Joinmap4.0 software with the maximum likelihood method.

Prediction of the candidate gene and sequence analysis

After identifying the polymorphic markers closely related to *Rfd1*, functional annotation of interval genes were obtained from JBrowse tool available through the Triticeae Multi-omics Center (http://202.194.139.32/jbrowse/). To acquire the full-length coding sequences of *Rfd1*, the specific primers were designed (Table S3) and *Rfd1* was cloned in Ju706A and LK783 using KOD DNA Polymerase (TOYOBO Co., Osaka, Japan). The purified PCR product was ligated into the *PBM16A* vector (Biomed Gene Technology Co., Beijing, China) and transformed into *Escherichia coli*. Subsequently, positive independent clones were picked and sequenced in TsingKe Biotechnology Co., Ltd (Beijing; http://www.tsingke.net). The sequence alignment was analyzed using DNAMAN software.

RNA extraction and expression analysis of candidate genes

Total RNA was extracted using RNA Extraction kit (Tiangen, Beijing, China) and first-strand cDNA was prepared using a PrimeScript First-strand cDNA Synthesis Kit (Roche, Switzerland). In order to determine expression level of candidate genes, qRT-PCR with 2 × Real Star Green Power Mixture (Gene-star Biosolutions Co., Beijing, China) was detected in QuantStudioTM Real-Time PCR System (Applied Biosystems, USA). Sequence-specific primers for qRT-PCR were designed using Triticeae Multi-omics Center (http://202.194.139.32/PrimerServer/) (Table S3). The qRT-PCR amplification conditions were as

follows: 95°C for 30 s; followed by 45 cycles of 95°C for 15 s, 60°C for 30 s. The *actin1* (GenBank: GQ 339766.1) for wheat was used as an internal control. The relative expression levels of the target genes were calculated using the $2^{-\Delta\Delta CT}$ method and each sample was performed in three technical replicates.

Subcellular localization

To determine the subcellular localization of Rfd1, The CDS of *Rfd1* without the stop codon was amplified and inserted into transient expression vector *pCAMBIA1302* with a green fluorescence protein (GFP) coding region to generate 35S:Rfd1-GFP, which was driven by the *cauliflower mosaic virus* (CaMV) 35S promoter. The 35S: GFP (control), 35S: Rfd1-GFP and cell membrane marker PIP2A-mCherry were transformed into the *Agrobacterium tumefaciens* GV3101 and then injected into the leaves of *Nicotiana benthamiana* plants (Sparkes et al. 2006). For plasmolysis treatment, 0.8 mol/L mannitol solution was used in this study. Fluorescence signals were visualized using a IX83- 167 FV1200 (Japan) confocal laser-scanning microscopy.

Plasmid construction for BSMV-VIGS and wheat infection

In order to verify the function of *Rfd1*, BSMV-VIGS experiment was carried out. The cDNA fragment (217bp) of *Rfd1* was selected to construct BSMV-VIGS vector and amplified in Ju783R by specific primers (Table S3). Viral vector construction and viral RNA transcription in vitro were as described (Yang et al. 2021). Transcripts in vitro including α/β/γ, α/β/γ-*TaPDS* and α/β/γ-*Rfd1* were mixed and diluted with FED solution to obtain three infective solutions: BSMV: 000, BSMV: *TaPDS* and BSMV: *Rfd1*. When the flag leaves were fully picked out, BSMV infective solution was applied to the flag leaf and the next leaf of wheat. After the infection, the phenotypes of leaves and anthers were observed by stereomicroscope (Motic, K4000). Total RNA was extracted from the anthers of uninfected, BSMV: 000-infected and BSMV: *Rfd1*-infected plants, and then transformed into cDNA for qRT-PCR. The determination of pectin content adopted the carbazole colorimetric method and the specific method referred to Yu et al. (1996). After the wheat matures, the seed setting rate was investigated:

seed setting rate (%) = (number of seeds per spike/spikelet number per spike)×100.

Construction of overexpression vector and *Arabidopsis* transformation

The first-strand cDNA of LK783 were used for PCR amplification and primers used for overexpression analysis were designed by Triticeae Multi-omics Center (http://202.194.139.32/PrimerServer/) (Table S3). Subsequently, the amplification product was cloned into *pCAMBIA1302* by *NcoI* and *SpeI* digestion and homologous recombinase ligation to generate *pCAMBIA1302: Rfd1*. The overexpression vector *pCAMBIA1302: Rfd1* was introduced into GV3101 (*Agrobacterium tumefaciens*) and transformation of *Arabidopsis thaliana* by the method of floral dip (Clough and Bent, 1998).

Seeds of the three *Rfd1*-overexpressing lines and wild-type were germinated on MS basal medium (0.22g MS powder + 0.75g sucrose + 0.8g agar) in growth chamber. Half of the seedlings were transplanted into

the soil, and the other half were collected for qRT-PCR. Relative expression levels for *Rfd1* in three transgenic lines were normalized using the *actin2* (GenBank: NC 003074.8) for *Arabidopsis* as standard. Morphological characteristics and alexander staining of pollen grains were observed by stereomicroscope (Motic, K4000).

Pollen germination assay in vitro

For wheat, mature anthers were put into the liquid pollen germination culture solution (20% sucrose + 10% PEG_{4000} + 40 mg/L H_3BO_3 + 3×10^{-3}mol/L Ca $(NO_3)_2$+10 mg/L VB1) at 28 ℃ incubated for 30 min. Then acetocarmine solution was added to observe and took pictures under stereomicroscope (Motic, K4000). For *Arabidopsis*, pollen grains of blooming flowers were shaken off on solid pollen germination medium (1 mM $Ca(NO_3)_2$+1 mM $CaCl_2$ + 1 mM $MgSO_4$ + 0.01%H_3BO_3 + 18% sucrose + 1.4% agar) at 28 ℃ incubated for 5 h. Then alexander solution was added to observe and capture pictures with stereomicroscope (Motic, K4000).

Statistical analysis

The data of all the above experiments were counted in the excel table, Student's t-test in the GraphPad Prism version 8.0.1 for Windows (GraphPad Software, San Diego, California USA, www.graphpad.com) were used to perform all statistical analyses. The values were designated as the means ± SD of three biological replicates per measurement.

Results

Ju706A, a male sterile line with *Aegilops Juvenalis* cytoplasm, performs complete male sterility with defective anther and pollen development

To observe the phenotypic characteristics of male sterile line Ju706A, the restorer line LK783 and their F_1, the florets and anthers from them were collected at the trinucleate stage (Tns). There was no significant difference in pistil between LK783 and Ju706A (Fig. 1a, d). However, compared with LK783, Ju706A displayed complete male sterility with indehisced anthers and aborted pollen grains, which were not dyed sufficiently with I_2-KI (Fig. 1b-c, e-f). In addition, the fertility of F_1 was normal when pollinated with LK783 as pollen ponors, indicating that the fertility of Ju706A can be restored by LK783 (Fig. 1g-i).

To further investigate the cytological differences between LK783 and Ju706A, SEM analysis was performed at the Tns. The result largely consistent with the above phenotypic characteristics, the Ju706A produced thin and shriveled anthers comparing with LK783 (Fig. 1j, q). In contrast to the neat and parallel cutin polymers on the outer epidermis of LK783, the outer epidermis of Ju706A was wrinkled and irregular in shape (Fig. 1k, l, r, s). The inner epidermis of both LK783 and Ju706A contained Ubisch bodies, but the Ubisch bodies arrangement of Ju706A were sparse and messy (Fig. 1m, n, t, u). Moreover, microspores of LK783 showed large and plump features, whereas Ju706A showed a small, shrunken

morphology (Fig. 1o, p, v, w). These results indicated the anthers and pollen development was disrupted in Ju706A.

Rfd1 is mapped to 2.4-Mb interval by BSA and 660K SNP array genotyping

To investigate the inheritance pattern of fertility restorer genes, Ju706A and LK783 were separately used as the female and male parents to construct BC_1F_1 populations. In segregation populations, there were a total of 506 plants: 232 sterile plants and 274 fertile plants. According to the χ^2 test, the BC_1F_1 population separation ratio was 1: 1 ($\chi^2 = 3.48 < \chi^2_{0.05,1} = 3.84$) (Table S1), thereby indicating that the fertility restorer character is controlled by single dominant gene locus (designed as *Rfd1*) from LK783. To map *Rfd1*, 326 SSR primers evenly distributed on 21 chromosomes of wheat were used to detect polymorphism in the two parents and two DNA pools (extremely sterile mixture pools and extremely fertile mixture pools). Consequently, nine polymorphic SSR primers (*Xgwm18*, *Xbarc137*, *Xwmc694*, *Xbarc061*, *Xcfd59*, *Xgpw1143*, *Xgpw4331*, *Xgpw3010*, *Xgpw4346*) located on chromosome 1B were identified and used to detect in 180 sterile individuals. The results showed that *Rfd1* was delimited in a 14.8 cM region between *Xgwm18* and *Xgpw1143* markers, which were closely linked to the *Rfd1* on 1BS (Fig. 2c, Table S2).

To further develop new polymorphic markers and narrow the target region, wheat 660K SNP array genotyping was carried out. In total, 23,086 differential SNPs (Used SNPs) were detected in the two parents and two DNA pools (Fig. 2a). Especially, 6,287 differential SNPs (27%) were located on chromosome 1B, which was the highest proportion among 21 chromosomes of wheat (Fig. 2b). Furthermore, according to the results of primary mapping, 50 pairs of SNP markers on chromosome arm 1BS were selected to confirm the fine mapping interval. Six markers (*AX-94768879*, *AX-95117169*, *AX-174254104*, *AX-111201011*, *AX-94793363*, *AX-111281507*) were found to exhibit polymorphisms both in parents and two DNA pools. Subsequently, polymorphic SNP markers were used to detect the recombinant plants among 232 sterile individuals. The linkage analysis results showed that *Rfd1*was narrowed to an approximately 2.4-Mb interval (134421108–136845581) between the SNP markers *AX-174254104* and *AX-111201011* (Fig. 2d, Table S2). Detection of partial polymorphic markers in sterile and fertile plants were shown in Fig. S1.

TraesCS1B02G197400LC is a strong candidate gene for *Rfd1*

According to the physical distance of the linkage markers, 19 genes were predicted to be located between *AX-174254104* and *AX-111201011* markers using the Triticeae Multi-omics Center (http://202.194.139.32/jbrowse/) (Fig. 2e, Table S4). In addition, 1,356 differentially expressed genes (DEGs) were filtered based on the RNA-Seq data of Ju706A and LK783. Four DEGs, comprising *TraesCS1B02G197400LC, TraesCS1B02G115300, TraesCS1B02G115400, TraesCS1B02G115500*, were screened in the candidate interval (Fig. 3a, Table S4). To identify candidate genes for *Rfd1*, qRT-PCR assay of these four DEGs was performed using RNA from different tissues (root, stem, leaves, anthers) and different developmental stages of anthers (Euns, Luns, Bns, and Tns). The results showed that *TraesCS1B02G115300, TraesCS1B02G115400*, and *TraesCS1B02G115500* had similar expression trends,

which were expressed in various tissues and the highest in roots. However, *TraesCS1B02G197400LC*, a gene encoding a pectinesterase, was the highest expressed in anthers at the Tns (Fig. 3b-f).

To understand the sequence differences between Ju706A and LK783, the full-length encoding sequence of *TraesCS1B02G197400LC* was isolated from Ju706A and LK783. It is characterized by 1350bp with only one exon and encodes 449 amino acids, a 7-bp deletion (CGGGGGC) was occurred at the 1176 bp in Ju706A, resulting in a frameshift mutation at the 393th amino acid (Fig. S2, Fig. S3). Taken together, T*raesCS1B02G197400LC* was suggested as a strong candidate gene for *Rfd1*.

Rfd1 is localized in the cell wall

To determine the subcellular localization of Rfd1, the 35S: GFP (as the control) and 35S: Rfd1-GFP were constructed (Fig. 4a) and transiently expressed in the leaves of *N. benthamiana*. The results indicated the 35S: GFP signals were expressed throughout the cell (Fig. 4b), while 35S: Rfd1-GFP signals were observed in the cell membrane or cell wall (Fig. 4c). To further verify the localization of Rfd1, *Agrobacterium tumefaciens* containing cell membrane marker PIP2A-mCherry and 35S: Rfd1-GFP was co-infiltrated into tobacco leaves. The co-expressed results showed that the GFP signals of 35S: Rfd1-GFP overlapped with the RFP signals of membrane marker PIP2A-mCherry (Fig. 4d). In the plasmolyzed cells, 35S: Rfd1-GFP signals were observed in the cell wall and PIP2A-mCherry signals in the cell membrane (Fig. 4e). These results indicated that the Rfd1 is localized in the cell wall.

Silencing of *Rfd1* leads to decreased fertility

To identify the function of *Rfd1* in wheat, BSMV-VIGS assay was performed on the restorer line Ju783R carrying the restorer genes *Rfd1Rfd1*. When the flag leaves of Ju783R were fully picked out, flag leaves were inoculated with BSMV: 000, BSMV: *TaPDS* and BSMV: *Rfd1*, respectively. The results showed that leaves of the uninfected plants were normal dark green, the leaves of BSMV: 000 plants appeared stripes and the leaves of BSMV: *TaPDS* plants displayed photobleaching, which indicated that the silencing of gene was effective. In addition, severely streaked leaves emerged in BSMV: *Rfd1*-infected plants (Fig. 5a). Compared with the normal florets and anthers in control, including uninfected, BSMV: 000 and BSMV: *TaPDS* plants, BSMV: *Rfd1* plants exhibited skinny florets and indehisced anthers (Fig. 5b, Fig. S4a). Furthermore, to determine the silencing effect of *Rfd1*, qRT-PCR assay and seed setting rate investigation were performed. Compared with the control plants, the expression of *Rfd1* was remarkably reduced in BSMV: *Rfd*1 plants (Fig. 5f). The seed setting rate reached more than 80% in the control plants, while there was less than 40% in BSMV: *Rfd1* plants (Fig. 5c, g). In addition, due to the decreased expression of *Rfd1*, the normal degradation of pectin was hindered, so that the pectin content of BSMV: *Rfd1* plants was higher than that of the control (Fig. 5h).

To investigate the causal factor responsible for the decreased seed-setting rate of the BSMV: *Rfd1* plants, the pollen vitality was observed. The results showed that the pollen grains of the control plants were completely fertile. However, the pollen grains of BSMV: *Rfd1* plants showed incomplete staining (Fig. 5d), displayed reduced pollen germination rate (Fig. 5e, i), contained two abnormal round sperm nuclei and a

vague vegetative nucleus (Fig. S4b), and presented small and shrunken morphology (Fig. S4c). Therefore, the above results indicated that the silencing of *Rfd1* affected pollen vitality and effectively reduced fertility.

Silencing of *Rfd1* exhibits abnormal development of anthers and microspores

To further explore the causes of male sterility, SEM and TEM observations were performed at the Tns. SEM showed that the anthers of the control plants were large and dehisced, and the outer epidermis of the anthers was highly defined with relatively glossy (Fig. S5a-b, d-g). By contrast, the anthers of BSMV: *Rfd1* plants failed to split and the outer epidermis was scattered and wrinkled. (Fig. S5c, h, i). Moreover, The Ubisch bodies were relatively sparsely arranged on the inner epidermis and the microspores were deformed and shrunken in the BSMV: *Rfd1* plants compared with control plants (Fig. S5j-u).

Additionally, TEM was applied to observe the dynamic process of anthers development from the Euns to Tns. At the Euns, there were no remarkable morphological differences in tapetum and microspore development between BSMV: 000 and BSMV: *Rfd1* plants. At the Luns, the tapetum layer of BSMV: 000 plants began to degrade, while BSMV: *Rfd1* plants were less degraded compared with BSMV: 000 plants. At the Bns, the tapetum layer continued to degrade, but the tapetum layer of BSMV: *Rfd1* plants was still thicker than that of BSMV: 000 plants. Until the Tns, the tapetum layer of BSMV: 000 plants was almost completely degraded with leaving only cell residues and the pollen grains were released from the ruptured pollen wall; whilst BSMV: *Rfd1* plants had a visible tapetum layer and the anther locule remained closed with no pollen release (Fig. 6a, b, Fig. S6a, b). Simultaneously, development of microspores and microspore walls were also observed. The microspore walls contained the intine layer and the exine layer including tectum, baculum and nexine. At the Euns, the microspores and microspore walls development in the BSMV: 000 plants was equivalent to that of the BSMV: *Rfd1* plants. From the Luns and Tns, The microspores of BSMV: *Rfd1* plants were shrunk and the exine of the anthers was arranged irregularly accompanied by abnormal accumulation of sporopollenin compared with BSMV: 000 plants. (Fig. 6c, d, Fig. S6c, d). Taken together, electron microscopy results suggested that *Rfd1* is required for anther development, tapetum degradation and microspore wall formation.

Heterogeneous expression of *Rfd1* promoted pollen germination in *Arabidopsis thaliana*

To further explore the function of *Rfd1*, an overexpression vector was constructed and three independent transformants (OE-*Rfd1*-3, OE-*Rfd1*-8 and OE-*Rfd1*-17) were obtained (Fig. 7a, b, c). To observe pollen activity, alexander staining and pollen germination in vitro were performed. The results showed that pollen grains of both wild type plants and overexpressed lines could be fully stained with alexander solution (Fig. 7e), but in the pollen germination experiment, the pollen germination rate was 64.6% in wild type plants, while the results in overexpressed lines were significantly increased from 72–84.1% (Fig. 7d, f).

In addition, compared with the wild type plants, the overexpressed lines showed delayed mossy and flowering, and the number of rosette leaf increased significantly (Fig. S7a, c). At 40 days, overexpressed

plants were observed to have more inflorescence side branches (2–4) and tended to grow simultaneously with the main stem (Fig. S7b, d). These results indicated that heterogeneous expression of *Rfd1* affected the vegetative growth and promoted pollen germination in *Arabidopsis thaliana*.

Development of molecular markers

Based on the 7 bp deletion of *TraesCS1B02G197400LC* in Ju706A, an InDel marker, *Xnwafu1*, was developed for molecular marker-assisted selection. Here, 180 sterile plants of BC_1F_1 population, 203 restorer lines and 41 maintainer lines were used to verify the accuracy of *Xnwafu1* marker. The results of polyacrylamide gel electrophoresis showed that there were no products in the sterile plants and maintainer lines, but the restorer lines had products at 260 bp. The *Xnwafu1* can identify all sterile plants (100%) in BC_1F_1 populations, 40 maintainer lines (97.6%) and 190 restorer lines (93.4%). Furthermore, 293 materials from different regions of China were used for fertility identifications and marker detection assays. According to results of fertility identifications (seed setting rate of F_1 is higher than 60% was considered fertile) and *Xnwafu1* marker test, the identification rate of the marker was 70.3% (Table S5, Fig. S8). Hence, *Xnwafu1* can be used as a good molecular marker for molecular marker-assisted selection of restorers.

Discussion

BSA combined with SNP array genotyping to accelerate gene mapping

Bulked segregant analysis (BSA) is an important method to identify genetic variants related to target genes and BSA combined with RNA sequence (RNA-seq) has been an efficient gene mapping technology which can accurately locate the target gene (Abe et al. 2012; Trick et al. 2012; Nestler et al. 2014; Ramirez-Gonzalez et al. 2015; Garcia et al. 2016; Singh et al. 2016; Du et al. 2017; Li et al. 2018; Sun et al.2018; Wang et al. 2018). Besides, BSA coupled with resequencing has been a rapid way to identify many important genes (Takagi H et al. 2013; Fletcher RS et al. 2016; Zhang et al. 2017; Tan et al. 2018; Wei et al. 2019). In recent years, the combination of BSA and SNP array genotyping technique has become more and more mature, and become a widely used technology in gene mapping. Wheat 9K array (Cavanagh et al. 2013), 90K array (Wang et al. 2014) and 660K array (Jia and Zhao. 2016) are used for gene mapping in wheat. Especially, wheat 660K array is the chip with the highest SNP density and it has been widely used in marker development (Jin et al. 2016; Li et al. 2017; Wu et al.2018; Zhai et al.2018). In this study, we used the wheat 660K genotyping technology combined with the BSA to develop SNP markers and narrow the restorer gene to the 2.4-Mb interval. Thus, the availability of the next-generation technologies and high-throughput SNP genotyping platforms greatly advanced gene mapping and cloning in wheat.

TraesCS1B02G197400LC encodes a PME, which may be involved in pollen wall formation and pollen tube germination

TraesCS1B02G197400LC encodes PME, which is an important enzyme in plant cell wall development. In plants, the abnormal development of the pollen wall can lead to male sterility. In *Arabidopsis*, the *ms2*

mutant displays defective exine layer and anomalous sporopollen accumulation process, leading to male sterility (Aarts et al.1997). The mutation of *DEX1* exhibits delayed the exine formation, damaged cell membrane structure and disorganized sporopollenin accumulation, resulting in male sterility (Paxson-Sowders et al.1997; 2001). The mutant *ms33* shows advanced inner wall formation and declined fertility (Fei and Sawhney 2001). In this study, the silencing of *Rfd1* exhibits skinny and shrunken pollen grains, scattered and irregular exine, and aberrant sporopollenin accumulation, causing the pollen wall defect.

In previous studies, it is found that the apical region of pollen tube is almost composed of a pectin network structure. Most of the esterified pectin exist in the apical region of the pollen tube to maintain the growth of the pollen tube, while the deesterified pectin is more concentrated in the area far away from the apical (Bosch et al. 2005b; Qun et al. 2007). Therefore, PME was also reported to participate in pollen development, pollen tube germination and growth. In *Arabidopsis thaliana* genome, there are 67 PME genes, of which at least 18 genes are highly expressed in pollen (Pina et al. 2005). In particular, *AtPPME1*and *VGD1* encoding a PME play an important role in pollen tube growth (Jiang et al. 2005; Tian et al. 2006). In cabbage, antisense transgenic plants of *BcMF3* display pollen abortion and the decreased germination rate (Wang et al. 2004; Liu et al. 2006). In maize, *ZmGa1P* encoding a pollen-specific PME regulates pollen tube growth (Zhang et al. 2018). Moreover, the coordinated action of PME and PMEI participates in pollen germination and pollen tube growth (Shi and Yang et al. 2010). In this study, pollen germination experiments were conducted on wheat and *Arabidopsis thaliana*, the pollen grains of *Rfd1* silencing plants in wheat hardly germinated, while overexpress of *Rfd1* in *Arabidopsis thaliana* promoted pollen tube germination and growth. Therefore, *Rfd1* may have an indelible role in pollen wall formation and pollen development.

Confirming function of *Rfd1* based on BSMV-Virus induced gene silencing

Virus induced gene silencing (VIGS) is a rapid and high-throughput technology for identifying gene functions. Recently, BSMV-VIGS has been widely used in the functional research of genes related to plant growth and development, stress resistance and disease resistance. BSMV-VIGS is the first time to establish and induce the silencing of *Lr21, Hsp90, RAR1* and *SGT1* in wheat, identifying that *Lr21* has the function of wheat stripe rust resistance (Scofield et al.2005). The function of *PDS* and *GFP* in *Dasypyrum villosum* is successfully silenced by BSMV-VIGS (Wang et al. 2009). BSMV-VIGS system is also successfully used in barley (Hein et al. 2005), *Brachypodium distachyon* (Demircan and Akkaya 2010), *Arabidopsis thaliana* (Manmathan et al. 2013), maize (Jarugula et al. 2018) and wheat (Yang et al. 2017; Han et al. 2021). In this study, to verify whether *TraesCS1B02G197400LC* was the candidate of *Rfd1*, BSMV-VIGS experiment was carried out. The results showed that the leaves of *Rfd1* silencing plants appeared white streaks, and the anthers were not dehisced. The I_2-KI staining, DAPI staining, aniline blue staining and pollen germination experiment all showed that the pollen grains were partially sterile. In addition, the seed setting rate and the gene expression level of *Rfd1* silencing plants were decreased compared with the control plants. These results demonstrated that the silencing of *Rfd1*can lead to partial loss of function and decreased fertility.

Fertility restoration in Ju706A is controlled by *Rfd1* derived from LK783

In recent years, fertility restorer genes for CMS have been mapped and cloned in various crops, such as sugar beet (Matsuhira et al. 2012), maize (Feng et al.2015), onion (Kim et al.2015), rice (Huang et al.2015), sorghum (Praveen et al. 2015). Apart from *Rf2* (encoded a mitochondrial glycine-rich protein) and *Rf17* (encoded a mitochondrial protein) in rice, *Rf2* (encoded a mitochondrial aldehyde dehydrogenase) in corn, *Rf1* (encoded a protein resembling OMA1) in sugar beet, the rest of the fertility restorer genes encode pentatricopeptide repeat (PPR) protein. It can be seen from the above that the diversity of fertility restorer genes may be due to the complex fertility restoration mechanism of CMS. Furthermore, there is a single locus on 1BS, Rf^{multi}, responsible for fertility restoration to *Ae. Kotschyi*, *Ae. Mutica* and *Ae. Uniaristata* cytoplasm (Tsunewaki 2015). However, the restorer *Rfk1* (*TraesCS1B02G197400LC*) located on 1BS chromosome against *Ae. Kotschyi* cytoplasm is a dominant gene locus derived from LK783, which differs from Rf^{multi} (Chen et al. 2021). In this study, *Rfd1* was mapped to a physical region of 2.4-Mb containing 19 candidate genes on chromosome 1BS. Furthermore, it was found that only *TraesCS1B02G197400LC* was highly expressed in anthers by RNA-Seq and qRT-PCR analysis. Coincidentally, we found that *TraesCS1B02G197400LC* was strongly expressed in the anther of LK783, but was weakly expressed in KTP116A and Ju706A (Fig. S9a, b). Nucleotide sequence alignment showed that both KTP116A and Ju706A had a 7 bp deletion (Fig. S9c, d). In addition, the molecular marker *Xnwafu-4* can also distinguish between LK783 and Ju706A (Fig. S9e). Thereby suggesting that Ju706A and KTP116A may have the same restorer locus derived from LK783.

Conclusion

In conclusion, fertility restorer locus for *Aegilops Juvenalis* cytoplasm in wheat, *Rfd1*, was mapped to physical intervals of 2.4-Mb on chromosome 1BS by BSA and 660K SNP array genotyping in BC_1F_1 population. *TraesCS1B02G197400LC* encoding a pectinesterase was identified as a candidate gene for *Rfd1*, which was strongly expressed in the anthers and its protein was localized in the cell wall. Down-regulation of *Rfd1* reduced pollen activity and affected the normal development of anther and microspores, leading to male sterility. Moreover, heterologous overexpression of *Rfd1* increased pollen vigor and affected vegetative growth. The research provided a good foundation for further study of fertility restoration mechanism in cytoplasmic male sterility with *Aegilops Juvenalis* cytoplasm.

Abbreviations

Bns, Binucleate stage

BSMV-VIGS, Barley stripe mosaic virus-induced gene silencing

Euns, Early uninucleate stage

Luns, Late uninucleate stage

SEM, Scanning electron microscopy

SNP, Singlenucleotide polymorphism

SSR,Simple sequence repeat

TEM, Transmission electron microscope

Tns, Trinucleate stage

Declarations

Acknowledgements

This work was supported by National Natural ScienceFoundation of China (32072060, 31771874).

Author contribution statement

XS and LZ conceived and designed the study. FN performed the experiments, analyzed the data, and wrote thearticle with contributions from all the authors.XS, YB,XY, YW and MHrevised and polished this manuscript. All authorshave read and approved the manuscript.

Conflict of interest

The authors declare no conflicts of interest.

Ethical standards

We declare that these experiments complied with the ethical standards in China.

Data availability statement

All data generated or analyzed during this study are included in this published article and its supplementary information files.

References

1. Aarts MG, Hodge R, Kalantidis K, Florack D, Wilson ZA, Mulligan BJ, Stiekema WJ, Scott R, Pereira A (1997) The *Arabidopsis* MALE STERILITY 2 protein shares similarity with reductases in elongation/condensation complexes. Plant J 12: 615-623
2. Abe A, Kosugi S, Yoshida K, Natsume S, Takagi H, Kanzaki H, Matsumura H, Yoshida K, Mitsuoka C, Tamiru M, Innan H, Cano L, Kamoun S, Terauchi R (2012) Genome sequencing reveals agronomically important loci in rice using MutMap. Nat Biotechnol 30: 174-178
3. Bosch M, ChEunsg AY, Hepler PK (2005a) Pectin methylesterase, a regulator of pollen tube growthPlant Physiol 138: 1334-1346

4. Bosch M, Hepler PK (2005b) Pectin methylesterases and pectindynamics in pollen tubes. Plant Cell 17: 3219-3226
5. Cavanagh CR, Chao S, Wang S, Huang BE, Stephen S, Kiani S, Forrest K, Saintenac C, Brown-Guedira GL, Akhunova A, etal (2013) Genome-wide comparative diversity uncovers multiple targets of selection for improvement in hexaploid wheat landraces and cultivars. Proc Natl Acad Sci U S A110: 8057-8062
6. Chen YR, Jia YL, Niu FQ, Wu YF, Ye JL, Yang XT, Zhang LL, Song XY (2021) Identification and validation of genetic locus *Rfk1* for wheat fertility restoration in the presence of *Aegilops kotschyi* cytoplasm. Theor Appl Genet 134:875-885
7. Clough SJ, Bent AF (1998) Floral dip: a simplified method for *Agrobacterium*-mediated transformation of*Arabidopsis thaliana*. Plant J 16: 735-743
8. Demircan T, Akkaya MS (2010) Virus induced gene silencing in *Brachypodium distachyon*, a model organism for cereals.Plant Cell Tissue & Organ Culture 100: 91-96
9. Dong X, Feng H, Xu M, Lee J, Kim YK, Lim YP, Piao Z, Park YD, Ma H, Hur Y (2013) Comprehensive analysis of genic male sterility-related genes in *Brassica rapa* using a newly developed Br300K oligomeric chip. PLoS One 8: 72178
10. Du H, Zhu J, Su H, Huang M, Wang H, Ding S, Zhang B, Luo A, Wei S, Tian X, Xu Y (2017) Bulked Segregant RNA-seq Reveals Differential Expression and SNPs of Candidate Genes Associated with Waterlogging Tolerance in Maize. Front Plant Sci 8: 1022
11. Fei HM, Sawhney VK (2001) Ultrastructural characterization of *male sterile33* (*ms33*) mutant in *Arabidopsis* affected in pollen desiccation and maturation. Can J Bot 79: 118-129
12. Feng Y, Zheng Q, Song H, Wang Y, Wang H, Jiang L, Yan J, Zheng Y, Yue B (2015) Multiple loci not only *Rf3* involved in the restoration ability of pollen fertility, anther exsertion and pollen shedding to S type cytoplasmic male sterile in maize. Theor Appl Genet 128: 2341-2350
13. Fletcher RS, Herrmann D, Mullen JL, Li Q, Schrider DR, Price N, Lin J, Grogan K, Kern A, McKay JK (2016) Identification of Polymorphisms Associated with Drought Adaptation QTL in *Brassica napus* by Resequencing.G3 (Bethesda) 6: 793-803
14. Fox T, DeBruin J, Haug Collet K, Trimnell M, Clapp J, Leonard A, Li B, Scolaro E, Collinson S, Glassman K, et al(2017) A single point mutation in *Ms44* results in dominant male sterility and improves nitrogen use efficiency in maize. Plant Biotechnol J 15: 942-952
15. Gaffe J, Tiznado ME, Handa AK (1997) Characterization and functional expression of a ubiquitously expressed tomato pectin methylesterase. Plant Physiol114: 1547-1556
16. Garcia V, Bres C, Just D, Fernandez L, Tai FW, Mauxion JP, Le Paslier MC, Bérard A, Brunel D, Aoki K, et al (2016) Rapid identification of causal mutations in tomato EMS populations via mapping-by-sequencing. Nat Protoc 11: 2401-2418
17. Guo P, Qi YP, Huang WL, Yang LT, Huang ZR, Lai NW, Chen LS (2018) Aluminum-responsive genes revealed by RNA-Seq and related physiological responses in leaves of two Citrus species with contrasting aluminum-tolerance. Ecotoxicol Environ Saf 158: 213-222

18. Hamawaki H, Mukai YT (1980) Mapping of the fertility-restoring gene *Rfv1*, against *Aegilops variabilis* cytoplasm in wheat. Jpn J Genet 55: 453-469
19. Han FQ, Yang C, Fang ZY, Yang LM, Zhuang M, Lv HH, Liu YM, Li ZS, Liu B, Yu HL, et al (2015) Inheritance and Indel markers closely linked to petal color gene (*cpc -1*) in *Brassica oleracea*.Mol Breed 35: 160
20. Han Y, Zhao F, Gao S, Wang X, Wei A, Chen Z, Liu N, Tong X, Fu X, Wen C, et al (2018) Fine mapping of a male sterility gene *ms-3* in a novel cucumber (*Cucumis sativus L.*) mutant. Theor Appl Genet 131: 449-460
21. Han Y, Zhao Y, Wang H, Zhang Y, Ding Q, Ma L (2021) Identification of ceRNA and candidate genes related to fertility conversion of TCMS line YS3038 in wheat. Plant Physiol Biochem 158:190-207
22. Hanson MR, Bentolila S (2004) Interactions of mitochondrial and nuclear genes that affect male gametophyte development. Plant Cell 16: S154-S169
23. Hein I, Barciszewska-Pacak M, Hrubikova K, Williamson S, Dinesen M, Soenderby IE, Sundar S, Jarmolowski A, Shirasu K, Lacomme C (2005) Virus-induced gene silencing-based functional characterization of genes associated with powdery mildew resistance in barley. Plant Physiol138: 2155-2164
24. Horn R (2006) Recombination: cytoplasmic male sterility and fertility restoration in higher plants. Springer Berlin Heidelberg pp 31–52
25. Huang TC, Zhang AM, Sun QX (1990) Overview and progress of hybrid wheat research in China. Crops 2: 5-7
26. Huang W, Yu C, Hu J, Wang L, Dan Z, Zhou W, He C, Zeng Y, Yao G, Qi J, et al (2015) Pentatricopeptide-repeat family protein RF6 functions with hexokinase 6 to rescue rice cytoplasmic male sterility. Proc Natl Acad Sci U S A 112: 14984-14989
27. Jarugula S, Willie K, Stewart LR (2018) Barley stripe mosaic virus (BSMV) as a vector in maize seedlings. Virus Genes 54: 616-620
28. Jia JZ, Zhao GY (2016) Wheat 660 SNP array developed by CAAS. http://wheat.pw.usda.gov/ggpages/topics/Wheat660_SNP_array_developed_by_CAAS.
29. Jiang L, Yang SL, Xie LF, Puah CS, Zhang XQ, Yang WC, Sundaresan V, Ye D (2005) VANGUARD1 encodes a pectin methylesterase that enhances pollen tube growth in the *Arabidopsis* style and transmitting tract. Plant Cell 17: 584-596
30. Jin H, Wen W, Liu J, Zhai S, Zhang Y, Yan J, Liu Z, Xia X, He Z (2016) Genome-Wide QTL Mapping for Wheat Processing Quality Parameters in a Gaocheng 8901/Zhoumai 16 Recombinant Inbred Line Population. Front Plant Sci 7: 1032
31. Ke LP, Sun YQ, Hong DF, LiuPW, Yang GS (2010) Identification of AFLP markers linked to one recessive genic male sterility gene in oilseed rape, *Brassica napus*. Plant Breeding124: 367-370
32. Kim S, Kim CW, Park M, Choi D (2015) Identification of candidate genes associated with fertility restoration of cytoplasmic male-sterility in onion (*Allium Cepa L.*) using a combination of bulked segregant analysis and RNA-seq. Theor Appl Genet 128: 2289-2299

33. Li MM, Li BB, Guo GH,Chen YX, Xie JZ, Lu P, Wu QH, Zhang DY, Zhang HZ, Yang J, et al (2018) Mapping a leaf senescence gene *els1* by BSR-Seq in common wheat. The crop J 6: 236-243
34. Liang Q, Wen D, Xie J, Liu L, Wei Y, Wang Y, Shi S (2014) A rapid and effective method for silver staining of PCR products separated in polyacrylamide gels. Electrophoresis 35: 2520-2523
35. Liu BS, Sun QX, Sun LZ,Gao QR, Zhang YC (2002) RAPD and ISSR markers of fertility restoring gene for *Aegilops kotschyi* cytoplasmic male sterility in wheat. Acta Botanica Sinica 44: 446-450
36. Liu DT, Zhang GS, Liu HW, Wang JW, Wang XL (1999) Research progress on fertility gene mapping of male sterility in wheat. Journal of Triticeae Crops 4: 6-11
37. Liu LC, Yu XL, Ye WZ, Xiang G, Cao JS (2006) Verification of antisense RNA function of male sterility related gene BcMF3 in Chinese cabbage. Journal of Zhejiang University 32:473-478
38. Liu ZH, Shi XY, Li S, Hu G, Zhang LL, Song XY (2018) Tapetal-Delayed Programmed Cell Death (PCD) and Oxidative Stress-Induced Male Sterility of *Aegilops uniaristata* Cytoplasm in Wheat. Int J Mol Sci19:1708
39. Manmathan H, Shaner D, Snelling J, Tisserat N, Lapitan N (2013) Virus-induced gene silencing of *Arabidopsis thaliana* gene homologues in wheat identifies genes conferring improved drought tolerance. J Exp Bot 64: 1381-1392
40. Matsuhira H, Kagami H, Kurata M, Kitazaki K, Matsunaga M, Hamaguchi Y, Hagihara E, Ueda M, Harada M, Muramatu A, et al (2012) Unusual and typical features of a novel restorer-of-fertility gene of sugar beet (*Beta vulgaris L.*). Genetics 192: 1347-1358
41. Melonek J, Duarte J, Martin J, Beuf L, Murigneux A, Varenne P, Comadran J, Specel S, Levadoux S, Bernath-Levin K, Torney F, Pichon JP, Perez P, Small I(2021) The genetic basis of cytoplasmic male sterility and fertility restoration in wheat. Nat Commun12: 1036
42. Mohr S (1993) Mitochondrial DNA of cytoplasmicmale-sterile *Triticum timopheevi*: rearrangement ofupstream sequences of the *atp6* and *orf25* genes.Theor Appl Genet 86: 259-268
43. Muhammad N, Zvobgo G, Zhang GP (2019) A review: The beneficial effects and possible mechanisms of aluminumon plant growth in acidic soil. Journal of IntegrativeAgriculture 18: 1518-1528
44. Murai K, Tsunewaiki K (1995) Photoperiod-sensitive cytoplasmic male sterility induced in Japanese wheatcultivars by transferring *Aegilops crassa* cytoplasm. Breed Sci 45: 199-203
45. Murai K, Tsunewaki K (1993) Photoperiod-sensitive cytoplasm male sterility in wheat with *Aegilops crassa* cytoplasm. Euphytica 67: 41-48
46. Nestler J, Liu S, Wen TJ, Paschold A, Marcon C, Tang HM, Li D, Li L, Meeley RB, Sakai H, et al (2014) Roothairless5, which functions in maize (*Zea mays L.*) root hair initiation and elongation encodes a monocot-specific NADPH oxidase. Plant J 79: 729-740
47. Nogueirol RC, Monteiro FA, Gratão PL, Borgo L, Azevedo RA (2015) Tropical soils with high aluminum concentrations cause oxidative stress in two tomato genotypes. Environ Monit Assess 187: 73

48. Panayotov.I (1980) New cytoplasmic male sterilitysources in common wheat: their genetical andbreeding consideration. Theor Appl Genet 56: 153-160
49. Paxson-Sowders DM, Dodrill CH, Owen HA, Makaroff CA (2001) DEX1, a novel plant protein, is required for exine pattern formation during pollen development in *Arabidopsis*. Plant Physiol 127: 1739-1749
50. Paxson-Sowders DM, Owen HA,Makaroff CA (1997) A comparative ultrastructural analysis of exine pattern development in wild type *Arabidopsis* and a mutant defective in pattern formation. Protoplasma 198: 53-65
51. Pina C, Pinto F, Feijó JA, Becker JD (2005) Gene family analysis of the *Arabidopsis* pollen transcriptome reveals biological implications for cell growth, division control, and gene expression regulation. Plant Physiol 138: 744-756
52. Praveen M, Anurag Uttam G, Suneetha N, Umakanth A, Patil JV, Madhusudhana R (2015) Inheritance and molecular mapping of *Rf6* locus with pollen fertility restoration ability on A1 and A2 cytoplasms in sorghum. Plant Sci 238: 73-80
53. Qun L, Ye D (2007) Roles of Pectin methylesterases in pollen-tube growth. *Journal of Intrgrative* Plant Biology 49: 94-98
54. Ramirez-Gonzalez RH, Segovia V, Bird N, Fenwick P, Holdgate S, Berry S, Jack P, Caccamo M, Uauy C (2015) RNA-Seq bulked segregant analysis enables the identification of high-resolution genetic markers for breeding in hexaploid wheat. Plant Biotechnol J 13: 613-624
55. Rausch T, Greiner S (2004) Plant protein inhibitors of invertases. Biochim Biophys Acta 1696: 253-261
56. Richard J, Noat G (1986) Electrostatic effects and the dynamics of enzyme reactions at the surface of plant cell. European Journal of Biochemistry 155: 183-202
57. Rockel N, Wolf S, Kost B, Rausch T, Greiner S (2008) Elaborate spatial patterning of cell-wall PME and PMEI at the pollen tube tip involves PMEI endocytosis, and reflects the distribution of esterified and de-esterified pectins. Plant J 53: 133-143
58. Scofield SR, Huang L, Brandt AS, Gill BS (2005) Development of a virus-induced gene-silencing system for hexaploid wheat and its use in functional analysis of the *Lr21*-mediated leaf rust resistance pathway. Plant Physiol 138: 2165-2173
59. Shi DQ, Yang WC (2010) Pollen germination and tube growth. Plant Developmental Biology-Biotechnological Perspectives 1: 245-282
60. Singh VK, Khan AW, Saxena RK, Kumar V, Kale SM, Sinha P, Chitikineni A, Pazhamala LT, Garg V, Sharma M, et al (2016) Next-generation sequencing for identification of candidate genes for Fusarium wilt and sterility mosaic disease in pigeonpea (*Cajanus cajan*). Plant Biotechnol J 14: 1183-1194
61. Sparkes IA, Runions J, Kearns A, Hawes C (2006) Rapid, transient expression of fluorescent fusion proteins in tobacco plants and generation of stably transformed plants. Nat Protoc 1: 2019-2025

62. Sun J, Yang L, Wang J, Liu H, Zheng H, Xie D, Zhang M, Feng M, Jia Y, Zhao H, Zou D (2018) Identification of a cold-tolerant locus in rice (*Oryza sativa L.*) using bulked segregant analysis with a next-generation sequencing strategy. Rice11: 24
63. Sun L (2001) RAPD analysing of CMS-T, K, V mtdnas and cloning of mtdna Fragments Associated with CMS-K in Wheat. Acta Agronomica Sinica27: 145-148
64. Takagi H, Abe A, Yoshida K, Kosugi S, Natsume S, Mitsuoka C, Uemura A, Utsushi H, Tamiru M, Takuno S, et al (2013) QTL-seq: rapid mapping of quantitative trait loci in rice by whole genome resequencing of DNA from two bulked populations. Plant J 74: 174-183
65. Tan C, Liu Z, Huang S, Feng H (2018) Mapping of the male sterile mutant gene *ftms* in *Brassica rapa L. ssp. pekinensis* via BSR-Seq combined with whole-genome resequencing. Theor Appl Genet 132: 355-370
66. Tan Y, Li S, Xie H, Duan S, Wang T, Zhu Y (2011) Genetical and molecular analysis reveals a cooperating relationship between cytoplasmic male sterility- and fertility restoration-related genes in *Oryza* species. Theor Appl Genet 122: 9-19
67. Tang JH, Fu ZY, Hu YM, Li JS, Sun LL, Ji HQ (2006) Genetic analyses and mapping of a new thermo-sensitive genic male sterile gene in maize. Theor Appl Genet 113: 11-15
68. Tian GW, Chen MH, Zaltsman A, Citovsky V (2006) Pollen-specific pectin methylesterase involved in pollen tube growth. Developmental Biology 294: 83-91
69. Trick M, Adamski NM, Mugford SG, Jiang CC, Febrer M, Uauy C (2012) Combining SNP discovery from next-generation sequencing data with bulked segregant analysis (BSA) to fine-map genes in polyploid wheat. BMC Plant Biol 12: 14
70. Tsunewaki K (1978) On the descent of the cytoplasms of polyploid species in triticum and aegilops. Proc. 5th Int. Wheat Genet. Symp 1
71. Tsunewaki K (2015) Fine mapping of the first multi-fertility-restoring gene, Rf^{multi}, of wheat for three *Aegilops* plasmons, using 1BS-1RS recombinant lines. Theor Appl Genet 128:723–732
72. Tsunewaki K, Mukai Y, Endo TR, Tsuji S, Murata M (1976) Genetic diversity of the cytoplasm in triticum and aegilops. Jpn.j.genet51: 175-191
73. Wang M, Wang G, Ji J,Wang J (2009) The effect of *pds* gene silencing on chloroplast pigment composition, thylakoid membrane structure and photosynthesis efficiency in tobacco plants. Plant Science 177: 222-226
74. Wang S, Wong D, Forrest K, Allen A, Chao S, Huang BE, Maccaferri M, Salvi S, Milner SG, Cattivelli L, et al (2014) Characterization of polyploid wheat genomic diversity using a high-density 90,000 single nucleotide polymorphism array.Plant Biotechnol J 12: 787-796
75. Wang Y, Zhang HZ, Xie JZ,Guo BM, Chen YX, Zhang HY, Lu P, Wu QH, Li MM, Zhang DY, et al (2018) Mapping stripe rust resistance genes by BSR-Seq: *YrMM58* and *YrHY1* on chromosome 2AS in Chinese wheat lines Mengmai 58 and Huaiyang 1 are *Yr17*. The crop J 6: 91-98

76. Wang YQ, Yu XL, Cao JS (2004) Isolation and characterization of *BcMF3*, a gene expressed only in maintainer line in Chinese cabbage-pak-choi (*Brassica campestris L.ssp.chinensis Makino var.communis Tsen et Lee*).Acta Genetica Sinica31: 1302-1308
77. Wei C, Wang H, Heng S, Wen J, Yi B, Ma C, Tu J, Shen J, Fu T (2019) Construction of restorer lines and molecular mapping for restorer gene of hau cytoplasmic male sterility in *Brassica napus*. Theor Appl Genet 132: 2525-2539
78. Wu J, Wang Q, Xu L, Chen X, Li B, Mu J, Zeng Q, Huang L, Han D, Kang Z (2016) Combining Single Nucleotide Polymorphism Genotyping Array with Bulked Segregant Analysis to Map a Gene Controlling Adult Plant Resistance to Stripe Rust in Wheat Line 03031-1-5 H62. Phytopathology 108: 103-113
79. Xiong X, Zhou D, Xu L, Liu T, Yue X, Liu W, Cao J (2019)*BcPME37c* is involved in pollen intine formation in *Brassica campestris*. Biochem Biophys Res Commun 517: 63-68
80. Yang W, Lou X, Li J, Pu M, Mirbahar AA, Liu D, Sun J, Zhan K, He L, Zhang A (2017) Cloning and Functional Analysis of MADS-box Genes, *TaAG-A* and *TaAG-B*, from a wheat K-type cytoplasmic male sterile line. Front Plant Sci 8:1081
81. Yang XT, Ye JL, Niu FQ, Feng Y, Song XY (2021) Identification and verification of genes related to pollen development and male sterility induced by high temperature in the thermo-sensitive genic male sterile wheat line. Planta 253:83
82. Yang XY, Zeng ZH, Yan JY, Fan W, Bian HW, Zhu MY, Yang JL, Zheng SJ (2013) Association of specific pectin methylesterases with Al-induced root elongation inhibition in rice. Physiol Plant 148: 502-511
83. Ye HT, Zhang MX, Xun CX, Zhao GW (2020)Cloning and functional analysis for the promoter of ZmMYB59 gene from maize (*Zea mays L.*). Journal of China Agricultural University 25: 23-30
84. Yu L, Love M(1996) Strawberry texture and pectin content as affected by electron beam irradiation. Journal of Food science 61: 844-846
85. Zhai S, Liu J, Xu D, Wen W, Yan J, Zhang P, Wan Y, Cao S, Hao Y, Xia X, Ma W, He Z (2018) A Genome-Wide Association Study Reveals a Rich Genetic Architecture of Flour Color-Related Traits in Bread Wheat. Front Plant Sci 9: 1136
86. Zhang AM, Huang TC (1997) Utilization and research progress of wheat heterosis. Crops 5: 16-20
87. Zhang GS, Yang TZ (1987) A preliminary report on 1B/1R wheat-rye male sterility of *Aegilops* cytoplasm. Shaanxi Journal of Agricultural Sciences 5: l -5
88. Zhang GS, Yang TZ (1989) A preliminary on the male sterile lines of wheat with *Ae.ventricosa,Ae.kotschyi* and *Ae.variabilis* cytoplasm. Acta Agronomica Sinica 15: 1-10
89. Zhang LL, Zhao FX, Xu AL (2002) Effective of *Ae.jevenalis* cytoplasm on Triticum. Acta Agricultural Boreali-Occidentalis11: 19-21
90. Zhang M, Lu X, Li C, Zhang B, Zhang C, Zhang XS, Ding Z(2018) Auxin Efflux Carrier *ZmPGP1* Mediates Root Growth Inhibition under Aluminum Stress. Plant Physiol 177: 819-832

91. Zhang X, Li R, Chen L, Niu S, Chen L, Gao J, Wen J, Yi B, Ma C, Tu J, Fu T, Shen J (2017) Fine-mapping and candidate gene analysis of the Brassica juncea white-flowered mutant *Bjpc2* using the whole-genome resequencing. Mol Genet Genomics 293: 359-370
92. Zhang Z, Zhang B, Chen Z, Zhang D, Zhang H, Wang H, Zhang Y, Cai D, Liu J, Xiao S, et al (2018) A PECTIN METHYLESTERASE gene at the maize *Ga1* locus confers male function in unilateral cross-incompatibility. Nat Commun 9: 3678

Figures

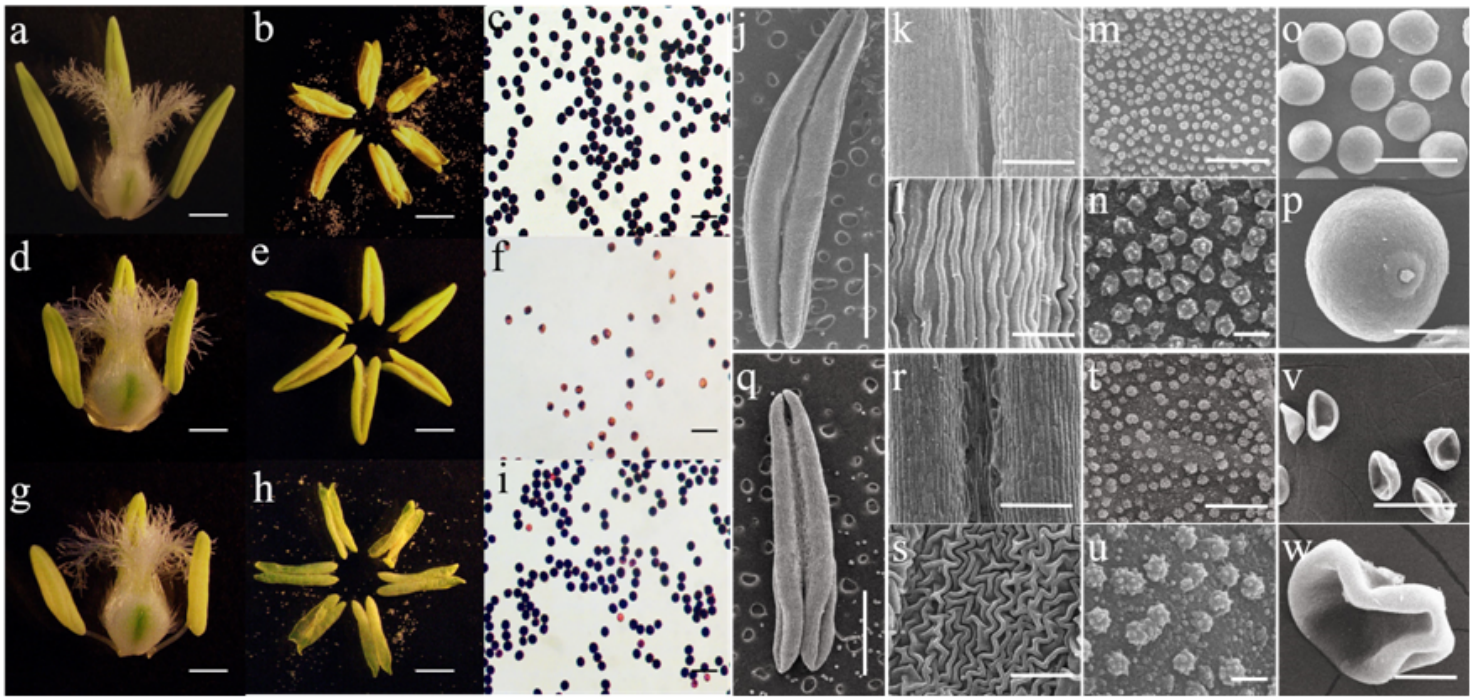


Figure 1

Phenotypic characteristics of LK783, Ju706A and F_1.**a-c, j-p** LK783; **d-f, q-w** Ju706A; **g-i** F_1; **a, d, g** Floret at thetrinucleate stage;**b, e, h, j, q** Anther at thetrinucleate stage; **c, f, i** I_2-KI staining of pollen grains; **k, l, r, s** Outer epidermis of anther at thetrinucleate stage; **m, n, t, u** Inner epidermis of anther at thetrinucleate stage; **o, p, v, w**Morphological observation of mature microspores. Scale bars = 1mm (**j, q**); 500μm (**a, b, d, e, g, h**); 100μm (**k, r**); 50μm (**c, f, i, o, v**); 10μm (**l, m, p, s, t, w**); 2μm (**n, u**).

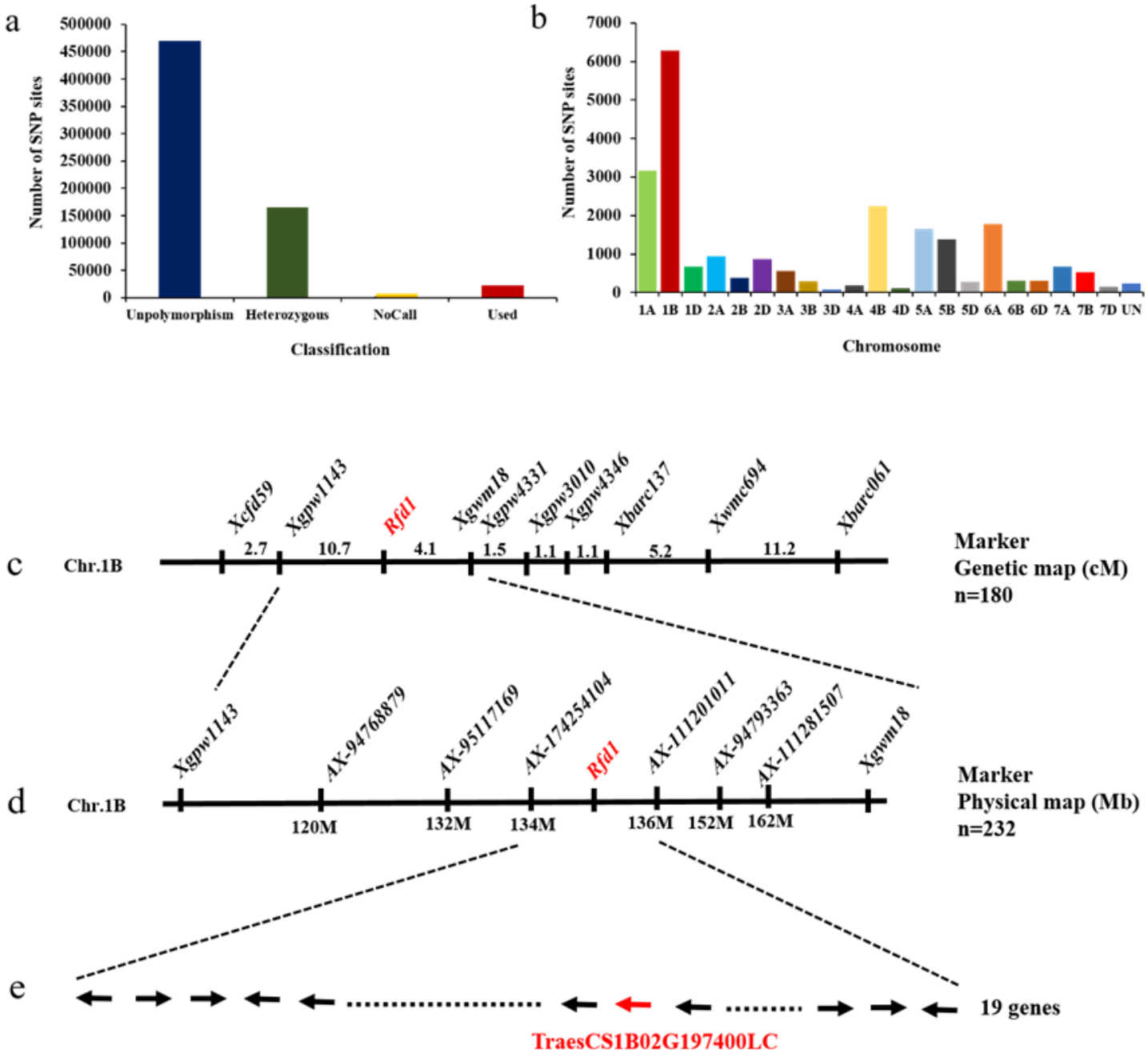


Figure 2

Fine mapping of the *Rfd1* by BSA and 660K SNP array genotyping. **a** Quality control of SNP data for 660K SNP array genotyping; Unpolymorphism, the number of unpolymorphism loci between the parents and DNA pools; Heterozygous, the number of heterozygous loci in the parent and DNA pools; Nocall, the number of sites where the typing success rate is less than 100%; Used, the number of loci used for differential SNP ratio analysis after filtering; **b**The distribution of differential SNPs on chromosomes; **c** Preliminary mapping of fertility restorer gene *Rfd1*,which was delimited in a 14.8 cM region between *Xgwm18* and *Xgpw1143* markers;**d**Fine mapping of fertility restorer gene *Rfd1*, whichwas narrowed to an 2.4-Mb interval between the SNP markers *AX-174254104* and *AX-111201011*; **e** Interval candidate gene.

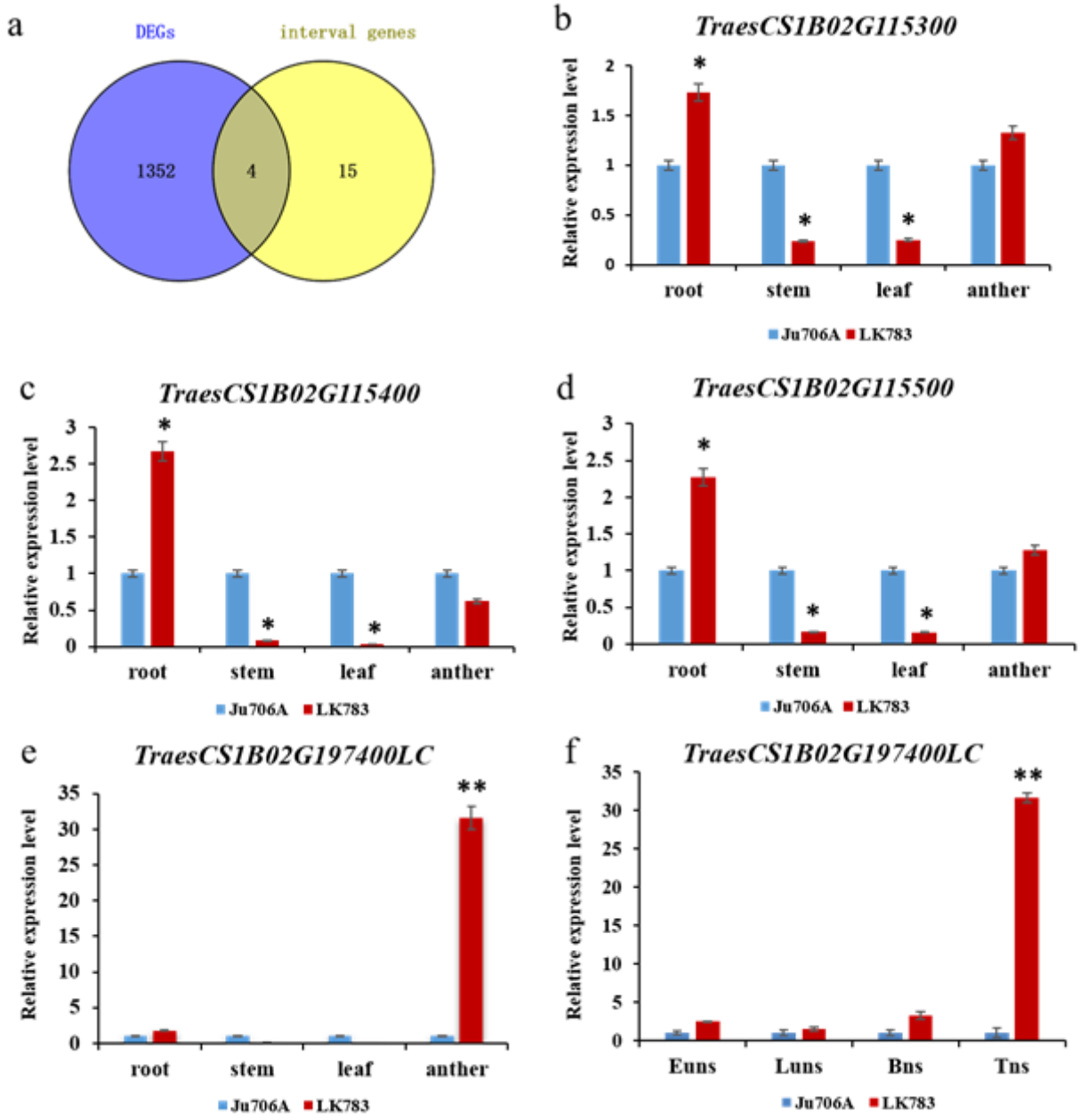


Figure 3

Expression analysis of candidate genes. **a** Venny diagram of differentially expressed genes (DEGs) and interval genes; **b** Expression analysis of *TraesCS1B02G115300* in different tissues; **c** Expression analysis of *TraesCS1B02G115400* in different tissues; **d** Expression analysis of *TraesCS1B02G115500* in different tissues; **e** Expression analysis of *TraesCS1B02G197400LC* in different tissues; **f** Expression analysis of *TraesCS1B02G197400LC* in anthers at different stages. Euns: early uninucleate stage; Luns: late uninucleate stage; Bns: binucleate stage; Tns: trinucleate stage.The ordinate represents $2^{-\Delta\Delta CT}$ values. The data obtained represent three replicates and bars represent standard deviation. Asterisks indicate significantly different data by T-test, * P<0.05, ** P<0.01.

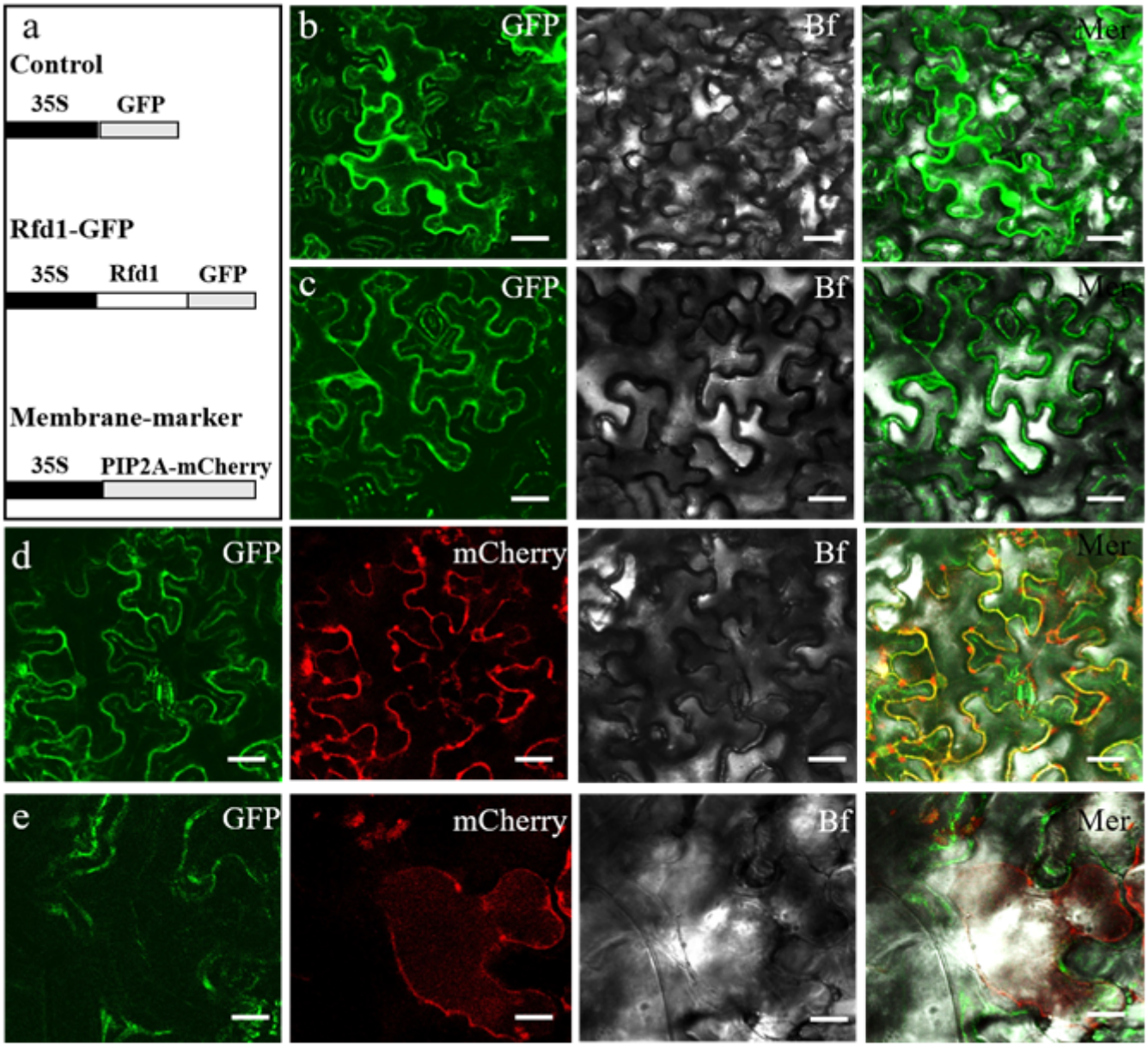


Figure 4

Subcellular localization of Rfd1 in tobacco leaf epidermalcells. Confocal images of tobacco leaf epidermal cells after 72 h ofinfection were shown. **a** The constructs for subcellular localization ofRfd1; **b** Transient expression of 35S: GFP (control); **c** Transient expression of 35S: Rfd1-GFP; **d**Co-expression of 35S: Rfd1-GFP and membrane marker PIP2A-mCherry; **e** Transient expression of plasmolyzed cells.Bf, brightfield; Mer, merged image of each channel; Scale bars = 20 μm.

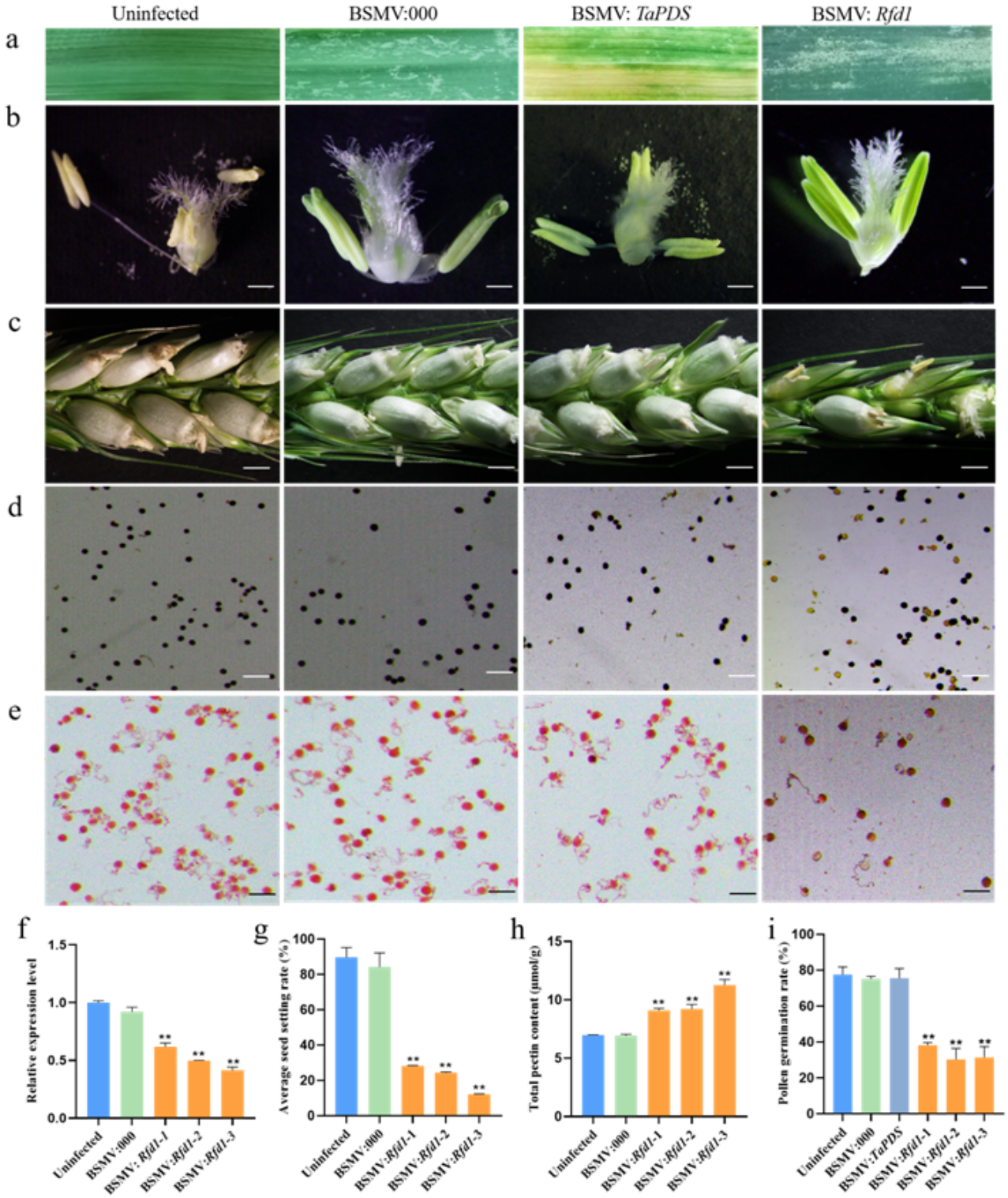


Figure 5

Phenotypic observation of control plants (uninfected, BSMV:000, BSMV: *TaPDS*) and BSMV: *Rfd1* plants for VIGS. **a**Phenotypic observation of leaf.; **b**Phenotypic observation of floret; **c**Phenotypic observation of spike; **d** I_2-KI staining of pollen grains at thetrinucleate stage; **e**Pollen germination experiment. Scale bars = 500μm (**a, b**); 200μm (**c**); 50 μm (**d, e**); **f** Relative expression analysis of *Rfd1*;**g** Investigation of seed setting rate; **h**Determination of pectin content;**i** Determination of Pollen germination rate. The data

obtained represent three replicates and bars represent standard deviation. Asterisks indicate significantly different data by T-test, * $P<0.05$, ** $P<0.01$.

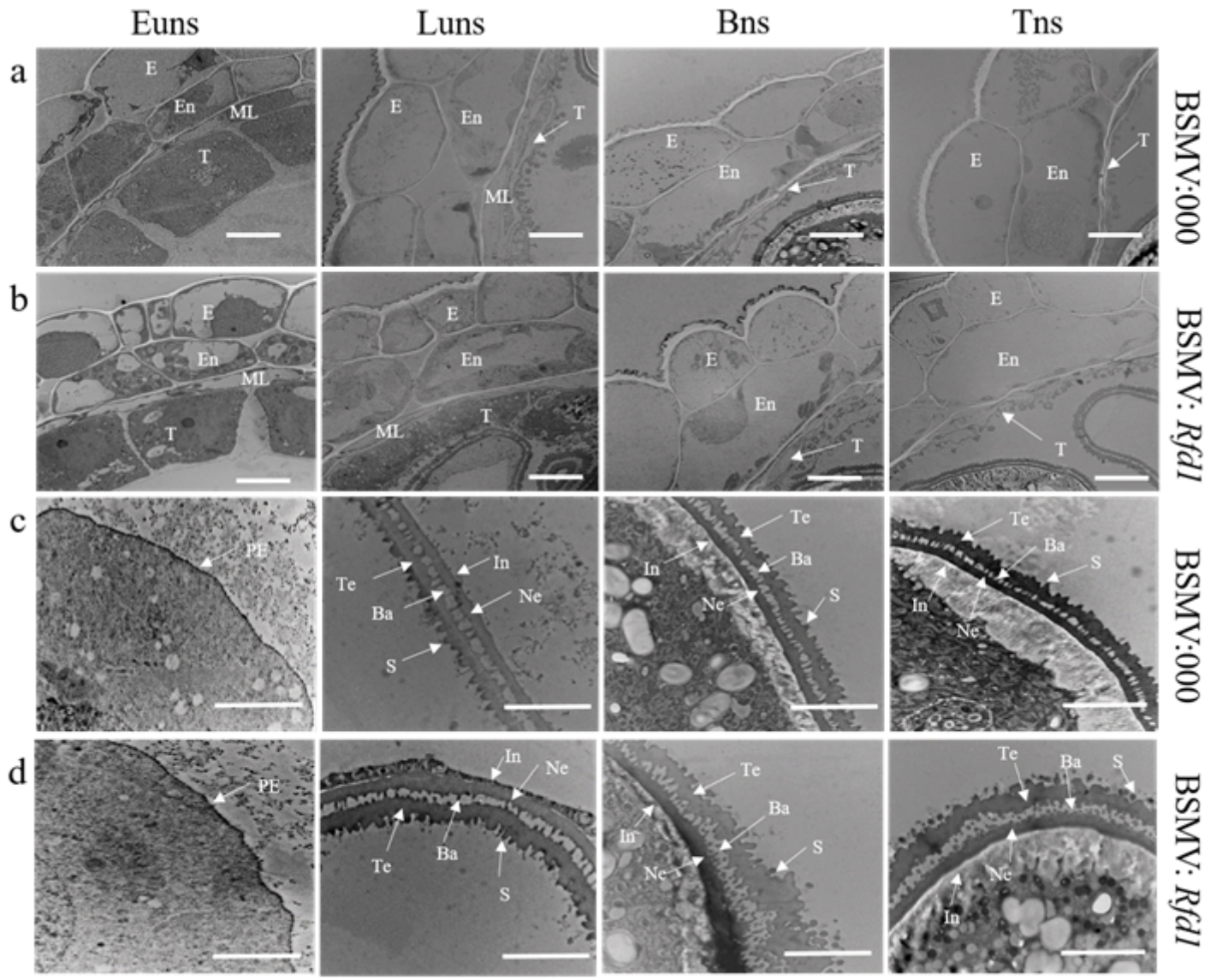


Figure 6

Transmission electron microscope observation of the tapetum layer and microspore wall in control plants (BSMV:000) and BSMV: *Rfd1* plants. **a, b**Ultrathin section observation of tapetum layer;**c, d**Ultrathin section observation of microspore wall. Euns: early uninucleate stage; Luns: late uninucleate stage; Bns: binucleate stage; Tns: trinucleate stage;E, En, ML and T represent Epidermis, Endothecium, Middle layer and Tapetum layer, respectively; PE,In, Ne, Ba, Te and S represent Primexine, Intine layer, Nexine, Baculum, Tectum and Sporopollenin, respectively;Scale bars = 2μm (**a-d**).

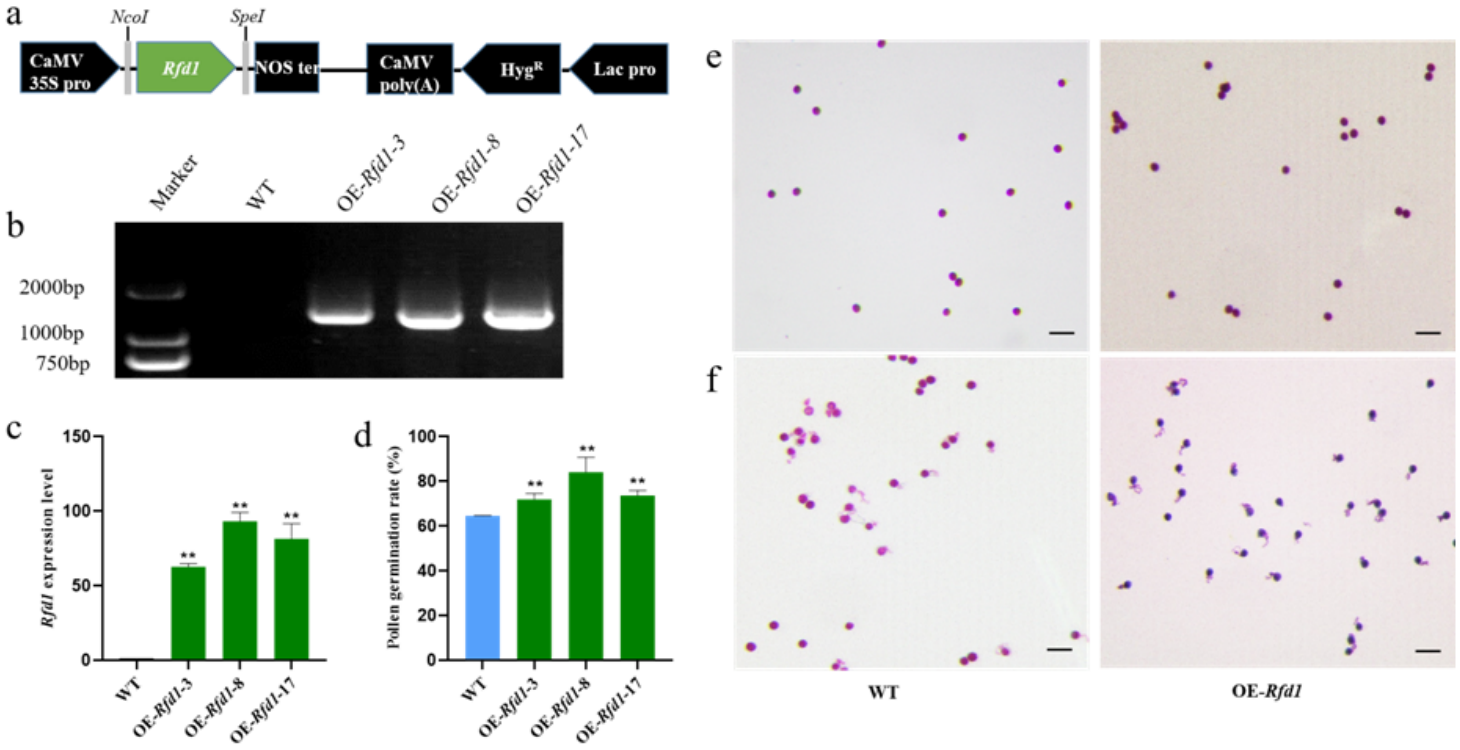


Figure 7

Identification of overexpressed plants and observation of pollen vigor. **a**Schematic diagram of overexpression vector;*NcoI* and *SpeI* were the restriction sites,Hygromycin (Hyg^R) was used as the selectable marker. **b**Identification of target fragment of T_3 transgenic plants.The transgenic plant had products at 1350bp, indicating that the target gene was successfully transferred into *Arabidopsis*; **c**Quantitative real-time PCR analysis of *Rfd1* gene expression level in wild-type and transgenic plants; **d**Investigation of pollen germination rate in wild type and transgenic plants.The data obtained represent three replicates and bars represent standard deviation. Asterisks indicate significantly different data by T-test, ** P<0.01. **e**Alexandrian staining of pollen grains; **f**Pollen germination assay in vitro.Scale bars = 50μm.

Supplementary Files

This is a list of supplementary files associated with this preprint. Click to download.

- FigureS1.docx
- FigureS2.docx
- FigureS3.docx
- FigureS4.docx
- FigureS5.docx
- FigureS6.docx

- FigureS7.docx
- FigureS8.docx
- FigureS9.docx
- TableS1.docx
- TableS2.xlsx
- TableS4.xlsx
- TableS5.xlsx